Multiple Andreev reflections in *s*-wave superconductor–quantum dot–topological superconductor tunnel junctions and Majorana bound states

Anatoly Golub
Department of Physics, Ben-Gurion University, Beer Sheva 84105, Israel
(Received 9 January 2015; revised manuscript received 17 April 2015; published 7 May 2015)

We calculate the current as a function of applied voltage in a nontopological *s*-wave superconductor–quantum dot–topological superconductor (TS) tunnel junction. We consider the type of TS which hosts two Majorana bound states (MBSs) at the ends of a semiconductor quantum wire or of a chain of magnetic atoms in the proximity with an *s*-wave superconductor. We find that the *I*-*V* characteristic of such a system in the regime of big voltages has a typical two-dot shape and is ornamented by peaks of multiple Andreev reflections. We also consider the other options when the zero-energy states are created by disorder (hereby Shiba states) or by Andreev zero-energy bound states at the surface of a quantum dot and a superconductor. The later are obtained by tuning the magnetic field to a specific value. Unlike the last two cases the MBS *I*-*V* curves are robust to change the magnetic field. Therefore, the magnetic-field dependence of the tunneling current can serve as a unique signature for the presence of a MBS.

DOI: 10.1103/PhysRevB.91.205105 PACS number(s): 71.10.Pm, 73.23.−b, 74.45.+c

I. INTRODUCTION

In recent years the exotic Majorana bound state (MBS) has been the focus of investigations in condensed-matter physics. Different platforms for obtaining a MBS and a variety of setups for experimental observation were suggested [1–9]. In particular a zero-bias peak in the conductance was predicted [10–13]. Recently [14] Majorana fermions where observed at the edge of a topological superconductor (TS) which was formed by a ferromagnetic chain placed in proximity to an *s*-wave superconductor with strong spin-orbital interaction. The other of the leading candidates is a semiconductor quantum wire in proximity to an *s*-wave superconductor—a system that generates a TS with two MBSs at its ends. A signature of a MBS in such a system has been detected in tunneling data in normal metal—TS junctions [15–17], although the evidence is not conclusive [18].

A setup has been suggested [19] for detecting an Aharonov-Bohm interference between the MBS and a quantum dot, predicting a structure in the tunneling data. Furthermore, zero-frequency shot noise has been studied [20–22]. However, more evidence of a MBS is needed.

The modified subgap features as signatures of the MBS due to multiple Andreev reflections (MARs) in a weak link between two topological superconductors was addressed in Ref. [23]. It has been shown theoretically that MARs in a weak link between two topological superconductors (i.e., hosting MBS) could cause novel subgap structures different from the trivial case which can also be regarded as signatures of the MBS [23,24]. The other more complicated setup was recently theoretically investigated in Ref. [25]. There the electronic transport through a junction where a quantum dot (QD) is tunnel coupled on both sides to semiconductor nanowires with strong spin-orbit interaction and proximity-induced superconductivity is analyzed.

Generally, the tunneling through quantum dots integrated in various tunneling systems has been a subject of considerable interest [26–33]. A possible probe for Majorana fermions was suggested in Ref. [26] where two MBSs that are coupled to quantum dots, which themselves interact with two normal-metal leads, can be uniquely tested by crossed Andreev reflection. The crossed Andreev reflection itself was proposed early in Ref. [34] as a method to probe nonlocality of a pair of MBSs. A simpler setup with a normal lead connected through one quantum dot to an MBS was analyzed in Ref. [27]. In this paper the nonlinear conductance as a function of applied bias and gate voltages was calculated in both cases of interacting and noninteracting QDs. The current peaks were used to read off the parity break of the Majorana system. The more complicated setup with one spinless quantum dot connected to two external normal leads and to the one end of a *p*-wave superconducting nanowire was considered in Ref. [28]. In this paper the peak value of conductance in a TS and nontopological phases was proposed as a method to detect MBSs.

The non-Abelian statistics of Majorana fermion states can be tested with the systems without quantum dots by studying the half quantum vortices in a two-dimensional chiral *p*-wave superconductor [35] or the fluxons' interferometry in a Josephson junction in a TS [36]. An interferometer for Majorana fermion edge states, which occur at an interphase between a superconductor and a magnet placed in the proximity of a topological insulator, was proposed in Ref. [37]. In this system the MBS transmission can be probed by charge transport. Separated MBSs in a network of nanowires in a topological phase have non-Abelian exchange statistics and were suggested for purposes of quantum computation [38]. To distinguish the MBS conductance peak from the zero-energy peak due to other effects (such as disorder) the tunneling in the presence of dissipation has been considered in Ref. [39]. Here the resistance of the lead is an important parameter that helps to identify MBS peak conductance as a function of temperature. Yet the other evidence for existence of the nanowire Majorana modes in a simple tunneling structure is based on the fact that nanowire Majorana modes always come in pairs [40]. Therefore, the hybridization due to finite-length wires leads to the splitting of the zero mode. It was shown [40] that this splitting has oscillatory dependence as a function of Zeeman energy or chemical potential.

The interacting quantum dot in the Kondo regime as a tunneling link between a normal lead and a MBS located at one end of the TS was considered in works [29–32]. Unlike the standard normal–quantum dot–normal (N-QD-N) tunneling systems, the Kondo effect in N-QD-TS junctions predicts a stronger temperature dependence of conductance at $T \gg T_K$ (T_K stands for Kondo temperature) [29,30,32]. This fact can by used for identification of a MBS. A setup with two normal leads and one QD connected to the Majorana zero mode of the TS was proposed to provide experiments which can probe Majorana physics by conductance and shot-noise measurements [33], wherein the dot may by in the Kondo regime.

Here we consider a simpler case of a tunnel junction s-wave superconductor–quantum dot–topological superconductor (S-QD-TS) where S stands for a topologically trivial s-wave superconductor and TS hosts one MBS at his tunneling end to the quantum dot. We study the case of large voltages V (although $eV < \Delta$) which permits ignoring constant phase difference. We use the approximation of a noninteracting dot ($U = 0$). This is justified if $T_K < \Delta$. In this case the Kondo effect has little impact on transport current. Moreover, we consider the low-temperature regime.

If interaction is small we assume that the charging energy of the dot is much smaller than Δ and may be ignored [41]. We also consider the weak tunneling limit when direct tunneling between superconductors is small and, therefore, multiple Andreev reflections due to these direct tunneling events are negligible in the subgap region.

Including the QD change in the situation: The transport current acquires a structure typical for two-dot tunneling processes [42]. However, we show that the contributions which come from a MBS of the TS can be easily distinguished from random impurity zero-energy states inside the gap of a topologically trivial s-wave superconductor. As an example of such an impurity we take classical magnetic impurity with spin S (Shiba model [43,44]). The Shiba resonance is strongly influenced by the applied magnetic field. The same is true in other cases of Andreev zero-energy bound states which we also consider in detail.

The structure of the paper is as follows. In Sec. II we introduce the model and present the Hamiltonian of the tunneling setup. In Sec. III we consider the case of a TS with Majorana bound states at the ends of the nanowire. Sections IV and V describe two other models without MBSs: the impurity zero mode (Shiba resonance) and Andreev zero-energy bound states, respectively. Finally, we conclude in Sec. VI. The techniques we include in Appendix.

II. THE HAMILTONIAN

The Hamiltonian of our system consists of the topologically trivial s-wave superconductor lead part H_L, the quantum dot H_d, and the tunnel couplings H_T Hamiltonian. The geometry is depicted in Fig. 1. Here t_R,t_L define the tunnel couplings between the MBS and the dot, between the dot and the lead. $N(0)$ is the density of states of the lead in the normal state, and the tunneling widths turn out to be $\Gamma_L = 2\pi N(0) t_L^2 \ll t_{L,R}$. The superconducting s-wave lead is placed at voltage bias V which is bigger compared to all other energy scales in the system, including Zeeman energy (although, V is less than the superconducting gap). We also assume that the MBS is well separated from other MBSs, e.g., at the other end of a TS wire, and therefore neglect the coupling between them. We write the Hamiltonian in spin (s matrices) and Nambu (particle-hole space, τ matrices) as

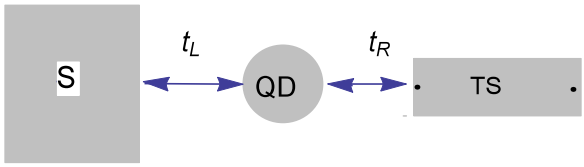

FIG. 1. (Color online) Structure of the tunneling junction which consists of a nontopological s-wave superconductor lead, an embedded quantum dot, and a topological superconductor with a Majorana fermion at its ends. The interaction couplings are presented. The phase is $\phi = 2eVt$ (we have dropped the constant phase).

$$\begin{aligned} H_d &= \tfrac{1}{2} d^\dagger(\varepsilon s_0 \tau_z + H s_z \tau_0) d, \\ H_T &= \tfrac{1}{2}[(t_L c^\dagger(0) + t_R \gamma \bar{V}^\dagger s_0)\tau_z d + \text{H.c.}, \end{aligned} \tag{1}$$

where s_0,τ_0,s_i,τ_i $(i = x,y,z)$ are unit and Pauli matrices, respectively, and $2H$ is the Larmor frequency, including the g factor. The Hamiltonian H_L of the superconducting lead has a standard form. The lead and dot electron operators are of the form $c = (c_\uparrow, c_\downarrow, c_\downarrow^\dagger, -c_\uparrow^\dagger)^T$, and the Majorana fermion operator γ comes with the spinor $\bar{V}_\varphi = (e^{i\varphi}, e^{i\varphi}, e^{-i\varphi}, -e^{-i\varphi})^T$, φ is the constant phase. The average energy level of the dot is ε.

Here we use a simplified form of interacting between the MBS and the QD suggested in Ref. [27]. In another model (model 2) which includes only interaction with one spin direction the first and last components of the spinor are replaced by zero (interacting with the down-spin of the dot). Model 2 may be relevant for strong magnetic fields.

The current operator is defined as $J = e\frac{d}{dt}N_L = -ie[N_L, H]$ and acquires a form $J = (-i/4) j_d$ where

$$j_d = t_L[c^\dagger(0)\tau_0 d - \text{H.c.}]. \tag{2}$$

We use the current in the Keldysh space [45,46] ($\hat{j}_d$) to construct the effective action with a source term. In the Keldysh theory the source field consists of two components: the classical α_{cl} and the quantum one α. The classical part α_{cl} is irrelevant for noise and current calculations, and we set it to zero. In this case the source action has a form

$$A_{\text{sour}} = \frac{1}{4}\int_t \alpha \hat{j}_d. \tag{3}$$

III. MAJORANA BOUND STATES AT THE ENDS OF THE TOPOLOGICAL SUPERCONDUCTOR

At first we consider a case with a TS as the right lead. The MBS states exist at both ends of a topological superconductor. For sufficiently long TS only one MBS is involved in tunneling. After integrating out the lead and dot operators we arrive at the effective action in terms of a Majorana Green's function (GF) which depends on coupling strengths and on quantum source

field $\alpha(t)$,

$$A_t = \frac{1}{2}\int_t \gamma^T G_M^{-1}\gamma, \quad G_M^{-1} = G_{M0}^{-1} - \Sigma(\alpha),$$
$$\Sigma(\alpha) = t_R^2 \hat{V}^\dagger \tau_3 G_d \tau_3 \hat{V}, \tag{4}$$

here $G_{M0}^{R,A}(E) = 1/(E \pm i\delta)$; the quantum dot GF $G_d(E) = [G_{d0}^{-1} - \Gamma_L g_T]^{-1}$ depends on left lead GF with included source term $g_T = T_- g T_+$, where

$$T_\pm = \tau_z\sigma_0 \pm \alpha\tau_0\sigma_x/2, \tag{5}$$

here $\sigma_{x,y,z}$ are the Pauli matrices in the Keldysh space. In the limit $\alpha \to 0$ we obtain

$$G_d(E) = \left[G_{d0}^{-1} - \Gamma_L \tau_3 g \tau_3\right]^{-1}. \tag{6}$$

The GF of the noninteracting dot in magnetic field H has a form

$$G_{d0}^R(E) = [(E + i\delta)s_0\tau_0 - \epsilon s_0\tau_z - H s_z\tau_0]^{-1}. \tag{7}$$

The Keldysh GFs of the lead,

$$g = \begin{pmatrix} g^R & g^K \\ 0 & g^A \end{pmatrix}, \tag{8}$$

in equilibrium ($V = 0$) g^R has a form

$$g^R = \frac{-i}{2}[a(E)s_0\tau_0 + b(E)s_0\tau_1], \tag{9}$$

$$a(E) = \frac{|E|\theta(|E| - \Delta)}{\sqrt{E^2 - \Delta^2}} + \frac{E\theta(\Delta - |E|)}{i\sqrt{\Delta^2 - E^2}}, \tag{10}$$

$$b(E) = \frac{\Delta}{E}a(E), \tag{11}$$

where $\theta(x)$ is a step function equal to one if $x > 0$ and is zero otherwise. The energy gap Δ describes the lead presented by a topologically trivial s-wave superconductor. Advanced function (A) is equal to the adjoint of the given retarded function; and $g^K(E) = [g^R(E) - g^A(E)]\tanh(E/2T)$.

The off-diagonal GF of an s-wave superconductor depends on the phase of the order parameter $\exp[\pm i\phi(t)] = \exp[\pm i2eVt]$. Therefore, at nonzero voltage V we have a Floquet periodic time-dependent problem with a basic frequency of $\omega_0 = 2eV$. A superconducting lead (topologically trivial) under a fixed voltage is described by time-dependent GFs. Their Fourier transforms are expressed in terms of equilibrium ones (a generalization to a 4×4 dimension of the relations from Ref. [47]),

$$g(E,E) = g_{11}(E - eV)s_0P_+ + g_{22}(E + eV)s_0P_-,$$
$$g(E,E - 2eV) = g_{21}(E - eV)s_0\tau_+,$$
$$g(E,E + 2eV) = g_{12}(E + eV)s_0\tau_-, \tag{12}$$

where $P_\pm = (\tau_0 \pm \tau_3)/2$, $\tau_\pm = \frac{1}{2}(\tau_x \pm \tau_y)$. The lead GF g may by any function (R, A, or K). We have dropped a constant phase which is justified for not very small voltages. A complete representation of GFs in the Floquet basis is presented in the Appendix.

We evaluate the current by taking derivatives of the effective action with respect to α and use dimensionless notations: All energies are taken in units of Δ. The total dc current is given by three contributions,

$$j/j_0 = \frac{t_R^2\Gamma_L}{2\Delta^3}(j_1 + j_2 + j_3), \tag{13}$$

where $j_0 = e/(2\Delta)$ and j_1, j_2, and j_3 are expressed in terms of a Majorana, a quantum dot, and left lead GFs (see the Appendix).

We calculate the I-V characteristics of a setup (Fig. 1) in the subgap region and consider zero and nonzero magnetic fields. It is known that in low transparency superconductor-normal metal-superconductor junctions the subgap current is small (approaching zero value) [24,47]. The tunneling through the dot between superconducting leads is responsible for MARs which contribute to the current. The MBS states, acting as the other dot, however, being structureless (mixing the spin) are quite robust to the change in magnetic field. Thus we have obtained characteristics (Fig. 2) typical for two-dot I-V curves [42]. However, unlike the nontopological case these I-V curves have different peak positions. In the whole subgap region current-voltage characteristics weakly depend on magnetic field. This is clearly reflected by Fig. 2: The peak position for three values of magnetic field: $H = 0$, 0.1Δ, and 0.2Δ practically coincide. This is a principal criterion which helps to identify the MBS.

The inset in Fig. 2 displays the I-V dependence for model 2. Here the current peak is shifted in comparison with the spin mixing model [Eq. (1)]. The magnetic-field dependence shows the bigger shift, although the peak's height is more suppressed. This difference comes out because in model 2 Majorana fermions do not mix the spins.

To calculate the I-V characteristics the number of Floquet states ($2n$) is adjusted until the result is insensitive to a further increase in n. The calculations include 12 Floquet states.

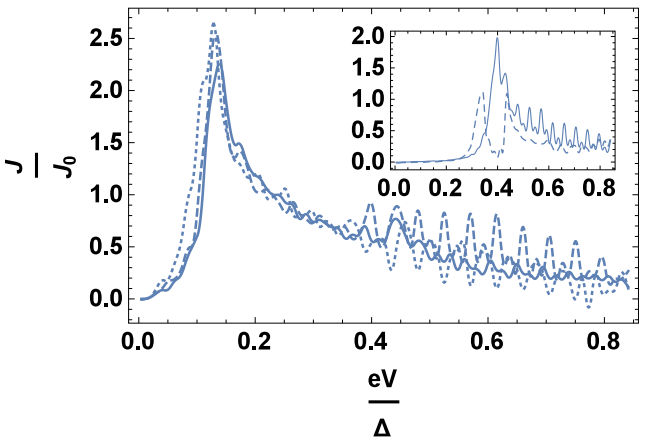

FIG. 2. (Color online) Current-voltage characteristics of the tunnel junction (Fig. 1). We set the dot energy $\epsilon = -0.01\Delta$, the temperature $T = 0.1\Delta$, and the tunneling widths $\Gamma_L/\Delta = 0.02$ and $t_R^2/\Delta^2 = 0.2$. The lines correspond to zero magnetic field (solid line), to $H = 0.1\Delta$ (dashed line), and $H = 0.2\Delta$ (dotted line). The inset: the current-voltage characteristics in model 2.

IV. IMPURITY ZERO MODE IN THE GAP (NO MBS)

To prove that we have a clear difference between topological and nontopological cases in this section we study the current for trivial topology but when, nevertheless, the zero bound states exist. This may be caused by Andreev bound states, by localized by disorder states (impurity), or by a surface state as in a d-wave superconductor [48]. We investigate the I-V characteristics in the case of single Shiba resonance [43,44] when it is tuned to form in-gap zero-energy bound states [49,50]. For a single impurity in the host superconductor lead (with $V = 0$) the scattering problem can be easily solved [43,44,49,50]. We consider a single (classical) magnetic impurity with spin S at the origin, interacting with the electron states,

$$H_{\rm imp} = -J\vec{S}c_R\bar{s}\tau_0 c_R(0),$$

where J is the exchange strength and c_R stands for the electron operator in the right superconductor. If we define the spin vector as $\vec{S} = S(\sin\theta\,\cos\phi, \sin\theta\,\sin\phi, \cos\theta)$, then at zero order in tunneling strength t_R, Green's function G_{s0} of the right lead acquires a form (in dimensionless units and for the frequencies less than the superconducting gap Δ, i.e., $|E| < 1$),

$$\begin{aligned}[2G^R_{s0}(E)]^{-1} = {} & \frac{E}{\sqrt{1-E^2}}s_0\tau_0 + \bar{\alpha}\,\cos\theta s_z\tau_0 \\ & - \frac{1}{\sqrt{1-E^2}}s_0\tau_x - Hs_z\tau_0 \\ & + \bar{\alpha}\,\cos\phi\,\sin\theta s_x\tau_0 \\ & + \bar{\alpha}\,\sin\phi\,\sin\theta s_y\tau_0, \end{aligned} \tag{14}$$

where $\bar{\alpha} = \pi N_R J S$ is the dimensionless impurity interaction and N_R is the density of electron states in the right lead. We did not take into consideration the Rashba spin-orbit interaction, although, the result for single impurity is similar to the case without spin-orbit scattering [50]. It was shown [49], and this can be directly checked by setting to zero the determinant of the matrix (14), that at $\bar{\alpha} \to 1$ and $H \to 0$ we arrive at the zero-energy bound states. In the low-energy domain close to the in-gap zero mode we can consider G_{s0} at small E. For voltages less than Δ this level defines transport. The tunneling interaction with the dot is described by the same Hamiltonian H_T (1) where instead of γV^+ we write projected to low-energy domain electron operator $f^\dagger$. As in the case of MBS we integrate out the electron operators of both the left lead and the quantum dot. Thus we arrive at a general form of the effective action and GF, which include interaction with the quantum dot,

$$G_s^{-1} = G_{s0}^{-1} - t_R^2 G_d. \tag{15}$$

The current consists of three contributions similar to those in Eq. (A15) however, there is an important difference: The Majorana GF is replaced by the GF of Shiba resonance G_s. In equilibrium $G^R_{s0}(E)$ (14) is a 4×4 matrix in spin and Nambu spaces. In the Floquet basis this matrix has a dimension of $4(1+2n)\times 4(1+2n)$, and the trace (see the Appendix) operates in this dimension. We calculate the current taking into consideration 12 Floquet states ($n = 6$) using the same set of parameters as in the case of the MBS. We consider several values of magnetic field: $H = 0$, 0.1Δ, 0.2Δ, and 0.3Δ. In Fig. 3 we see a shift in a peak of transport current as the magnetic field is changed. This does not occur in the MBS case [Eq. (1)]. Unlike the MBS case (Fig. 2), here the peak position shifts with Zeeman energy, and this dependence on H can serve as a possible method to distinguish the Shiba resonance from the MBS.

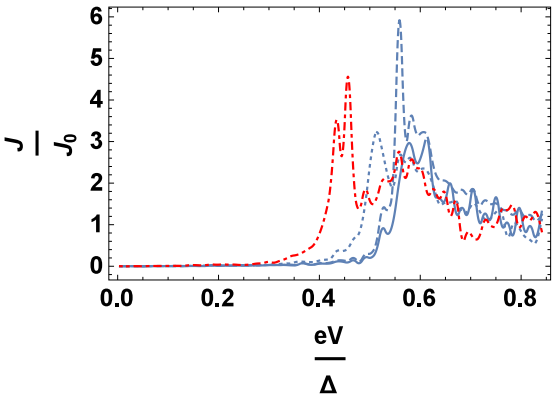

FIG. 3. (Color online) The same as in Fig. 2, where, however, the TS is replaced by Shiba resonance at $\bar{\alpha} \to 1$. For this figure we took direction angles: $\phi = 0$, $\theta = \pi/2$. The other parameters are as in Fig. 2 but in addition dot-dashed curve which corresponds $H = 0.3\Delta$ is included.

V. ANDREEV ZERO BOUND STATES

Andreev bound states can appear in a system, such as ours, when a quantum dot contacts with a superconductor. The zero-energy limit mimics the MBS and may be obtained by proper tuning the Zeeman energy. Let us consider setup, such as presented by Fig. 1 where, however, instead of a topological superconductor on the right-hand side, we have an s-wave superconductor which is grounded. By tuning the magnetic field we intend to get the low-energy subspace due to interaction with the s-wave superconductor, i.e., we associate Andreev zero bound states (AZBSs) only with an s-wave superconductor which couples to a quantum dot. Integrating out the electron operators of superconductors (left lead and right) we obtain a total GF G_t of the dot which includes interactions with both superconductors. Actually, G_t has a form of Eq. (6), although, G_{d0} is replaced by G_{t0},

$$\begin{aligned} G_{t0}^{-1R}(E) = {} & \left(E + \frac{\Gamma_R E}{2\sqrt{\Delta_R^2 - E^2}} + i\delta\right) s_0\tau_0 - \epsilon s_0\tau_z \\ & - Hs_z\tau_0 - \frac{\Gamma_R\Delta_R}{2\sqrt{\Delta_R^2 - E^2}}s_0\tau_x, \end{aligned} \tag{16}$$

where we, anticipating a low-energy domain, consider only the case of $|E| < \Delta_R$. It is a direct way to show (by finding the roots of equation $\det[G_{t0}^{-1R}] = 0$) that the zero-energy bound state can appear when we tune Zeeman energy to the value $H = H_0 = \sqrt{\Gamma_R^2/4 + \epsilon^2}$.

We compute the transport current (see Appendix) and find the I-V characteristics of the junction (Fig. 4). We can clearly distinguish AZBSs which are created at magnetic field

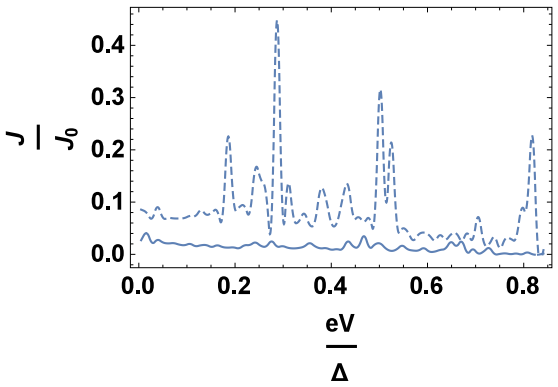

FIG. 4. (Color online) The tunneling current versus voltage in the case of formation of AZBS at $H = H_0$ (dashed curve) and at $H = 0$ when AZBSs are depressed (solid line). Here we have chosen the dot energy $\epsilon = -0.4\Delta$, the temperature $T = 0.03\Delta$, and the tunneling widths $\Gamma_L/\Delta = 0.2$ and $\Gamma_R/\Delta = 0.3$.

$H = H_0$ from the Andreev bound states created at $H \neq H_0$ (here $H = 0$). Many resonances which are shown in Fig. 4 correspond to a Floquet number shifted by the zero-energy pole of the GF (16). Moreover, although, the AZBS can mimic the resonance due to the MBS, this resemblance may be destroyed by a magnetic field different from H_0.

VI. CONCLUSION

We have applied the standard Keldysh technique [45,46] to evaluate the tunneling current in the setup as presented by Fig. 1. As a specific example we consider a Majorana fermion at the end of a quantum wire which is placed in proximity with a superconductor and under an applied external magnetic field [5,6]. Evidently, control of the magnetic field and the dot-MBS coupling t_R can provide a sensitive test for the MBS detection and may help to distinguish the MBS from other zero bound states [18] caused either by Andreev bound states or localized by disorder states or by surface states as in d-wave superconductors [48]. The difficulty with experimental identification of a MBS via the method of a zero-bias conduction peak [15–18] is that similar peaks may be due to other low-energy bound states [53], such as states localized by disorder [51]. However, in the experiment [14] a chain of interacting magnetic iron atoms (magnetic dots) on the superconducting lead was investigated. For this system which includes Hubbard interaction in the dot [52] the theory [51] is not directly applied.

We provide the solution of several models: two with the MBS, the other one is a model in which the MBS is replaced by Shiba impurity resonance, and the last model represents the AZBS that can appear at the contact of a quantum dot and an s-wave superconductor at the specific value of Zeeman energy. We consider multiple Andreev reflections which are beyond the small voltage regime. We show that for the last two (no MBS) models zero localized states may be identified by strong peak position dependence on the magnetic field. However, in model 2 of the MBS that describes the interaction of Majorana fermions with only one spin state of a QD (here spin-down) current peak decreases with magnetic field, although, unlike the model Eq. (1) it is shifted. Physically this happens because in the model [Eq. (1)] the interaction with spins of the dot involves spin mixing and Majorana fermions act like a Bogoliubov quasiparticle, whereas in model 2 spin mixing is excluded. A further difficulty with experimental identification is due to the accuracy with which a zero-energy state can be determined as a function, e.g., of a magnetic field [16,17,53,54]. Therefore, control of the magnetic field and the dot-MBS coupling t_R provides an option for a MBS detection.

ACKNOWLEDGMENTS

I would like to thank B. Horovitz for stimulating discussions. This research was supported by the ISRAEL SCIENCE FOUNDATION (BIKURA) (Grant No. 1302/11).

APPENDIX

1. Green's functions in Floquet space

Here we obtain the nonequilibrium GFs of the superconductor (left electrode), the Majorana, and the dot Green's functions [Eqs. (4) and (6)] as matrices in Floquet space. At constant applied voltage V the tunneling between two superconductors is described by GFs which depend on time via the phase of the order parameter [47]. The nonequilibrium GF of superconductor $\tilde{g}$ acquires a form

$$\tilde{g}(t,t') = \exp\left[\frac{i\phi(t)\tau_z}{2}\right] g(t-t') \exp\left[\frac{-i\phi(t')\tau_z}{2}\right], \quad \text{(A1)}$$

where $\phi(t) = \phi_0 + 2eVt$, ϕ_0 is a constant phase which we set to zero and $g(t-t')$ is the equilibrium GF of the superconductor. Due to off-diagonal terms in g the phase exponent does not commute with g. Therefore, the Fourier transform of $\tilde{g}$, which depends on two energies, includes energies shifted by a period of $2eV$, actually a multiple of this period (12),

$$\begin{aligned}\langle E|\tilde{g}|E'\rangle = {} & \delta(E-E')g(E,E) + \delta(E-E'-2eV) \\ & \times g(E,E-eV) + \delta(E-E'+2eV) \\ & \times g(E,E+eV). \end{aligned} \quad \text{(A2)}$$

The current is presented as a Fourier series $J(t) = \sum_n \exp[i2eVt]\hat{J}_n(2eV)$. The zero component ($n = 0$) stands for the averaged current which includes integration over E,E'. Therefore, all δ functions in (A2) are integrated out, and only functions $g(E,E')$ remain. If in these GFs we replace E,E' by $E + 2eVm, E + 2eVn$ then it is convenient to introduce the matrix notation: $g(E + 2eVm, E + 2eVn) = g_{m,n}(E)$. Because g for every m,n is a 4×4 matrix itself we use the indices i,k to designate the actual matrix element [47].

Let us consider $2N + 1$ Floquet states. As the simplest example we start with the zero-order retarded Majorana GF [see Eq. (4)]. It has no 4×4 matrix structure and thus consists of only diagonal matrix elements in Floquet space,

$$G^{-1R}_{M0p,q}(E) = \delta_{p,q}(E - 2eVN + 2eVp). \quad \text{(A3)}$$

Definitions of GFs [Eq. (12)] show that the energy difference between the initial and the final states is the integer multiple of $2eV$. To simplify notations we

define $I = \text{integer}[\frac{i-1}{4}]$, $K = \text{integer}[\frac{k-1}{4}]$, and $E_K = E - 2eV(N-K)$, where $i,k = 1,2,\ldots,4(2N+1)$. Thus we have

$$\begin{aligned} g_{i,k}(E) &= g_d[i,k] + g_+[i,k] + g_-[i,k], \\ g_d[i,k] &= \delta_{I,K}\{g_{11}(E_K - eV)s_0P_+ \\ &\quad + g_{22}(E_K + eV)s_0P_-\}_{i-4K,k-4K}, \\ g_+[i,k] &= \delta_{I,K-1}g_{21}(E_K - eV)\{s_0\tau_+\}_{i-4(K-1),k-4K}, \\ g_-[i,k] &= \delta_{I,K+1}g_{12}(E_K + eV)\{s_0\tau_-\}_{i-4(K+1),k-4K}. \end{aligned} \tag{A4}$$

The matrix structure of the $4(2N+1)\times 4(2N+1)$ matrix $g_{i,k}(E)$ consists of 4×4 diagonal boxes (g_d) and of 4×4 blocks $g_\pm$ on each side of the diagonal. The other Keldysh GFs have similar representations. The dot GF [Eq. (6)] includes the lead GF g as its nonequilibrium part, therefore, we can write the total inverse dot GF in the form, such as g [Eq. (A4)],

$$\begin{aligned} G^{-1R}_{di,k}(E) &= G_1[i,k] + G_+[i,k] + G_-[i,k], \\ G_1[i,k] &= \delta_{I,K}\{E_Ks_0\tau_0 - \epsilon s_0\tau_z - Hs_z\tau_0 \\ &\quad - \Gamma_L[g_{11}(E_K - eV)s_0P_+ \\ &\quad + g_{22}(E_K + eV)s_0P_-]\}_{i-4K,k-4K}, \\ G_+[i,k] &= \delta_{I,K-1}\Gamma_Lg_{21}(E_K - eV)\{s_0\tau_+\}_{i-4(K-1),k-4K}, \\ G_-[i,k] &= \delta_{I,K+1}\Gamma_Lg_{12}(E_K + eV)\{s_0\tau_-\}_{i-4(K+1),k-4K}. \end{aligned} \tag{A5}$$

The dot GF $G_{di,k}$ is obtained by taking the inverse of Eq. (A5).

The total Majorana GF, although, which depends on dot function G_d [Eq. (A4)], has no spin and particle-hole presentation. It is a matrix only in Floquet space $(2N+1)\times(2N+1)$. Using the definition of spinor $\hat{V_{\varphi=0}}$ [see Eqs. (1) and (4)] we find

$$G^{-1R}_{Mp,q}(E) = G^{-1R}_{M0p,q}(E) - \Sigma^R_{p,q}(E), \tag{A6}$$

$$\begin{aligned} &\Sigma^R_{p,q}(E) \\ &= t_R^2\{G^R_{d1+4p,1+4q}(E) + G^R_{d2+4p,2+4q}(E) + G^R_{d3+4p,3+4q}(E) \\ &\quad + G^R_{d4+4p,4+4q}(E) + G^R_{d1+4p,3+4q}(E) - G^R_{d2+4p,4+4q}(E) \\ &\quad + G^R_{d3+4p,1+4q}(E) - G^R_{d4+4p,2+4q}(E) - G^R_{d1+4p,4+4q}(E) \\ &\quad + G^R_{d2+4p,3+4q}(E) + G^R_{d3+4p,2+4q}(E) - G^R_{d4+4p,1+4q}(E) \\ &\quad + G^R_{d1+4p,2+4q}(E) + G^R_{d2+4p,1+4q}(E) \\ &\quad - G^R_{d3+4p,4+4q}(E) - G^R_{d4+4p,3+4q}(E)\}, \end{aligned} \tag{A7}$$

here $p,q = 0,1,2,\ldots,2N$. Inverting Eq. (A6) we arrive at the effective Majorana GF.

The inverse GF of the Shiba states in the low-energy limit close to the in-gap zero (at $\tilde{\alpha}=1$) replaces the Majorana GF $G_{M0p,q}(E)$ in the expressions for the tunneling current. The effective Shiba state Green's function [Eq. (15)] has the self-energy part which is determined by interaction with the dot. In the Floquet basis this GF is a $4(2N+1)\times 4(2N+1)$ matrix which has the form

$$G^{-1R}_{sp,q}(E) = G^{-1R}_{s0i,k}(E) - t_R^2G^R_{di,k}(E), \tag{A8}$$

$$\begin{aligned} G^{-1R}_{s0i,k}(E) &= \delta_{I,K}\{E_Ks_0\tau_0 - \epsilon s_0\tau_z - Hs_z\tau_z + \cos\theta s_z\tau_0 \\ &\quad + \cos\phi\,\sin\theta s_x\tau_0 + \sin\phi\,\sin\theta s_y\tau_0\}_{i-4K,k-4K}. \end{aligned} \tag{A9}$$

2. The tunneling current

Let us at first consider the tunneling current in the S-QD-TS (MBS) junction. We evaluate the current by taking derivatives of the effective action with respect to α,

$$j(t) = \frac{e}{4}\text{Tr}\int dt_1\int dt_2 G_M(t_1t_2)\left(\frac{\delta\Sigma(\alpha t_2t_1)}{\delta\alpha(t)}\right)_{\alpha\to 0}, \tag{A10}$$

where Tr acts in the Keldysh space. Explicitly the derivative acquires the form

$$\begin{aligned} \frac{\delta\Sigma(\alpha t_2t_1)}{\delta\alpha(t)} &= t_R^2\Gamma_L\int dt_3\int dt_4\hat{V}^\dagger G_d(t_2t_3)\frac{\delta g_T(t_3t_4)}{\delta\alpha(t)} \\ &\quad\times G_d(t_4t_1)\hat{V}, \end{aligned} \tag{A11}$$

$$\begin{aligned} \left(\frac{\delta g_T(t_3t_4)}{\delta\alpha(t)}\right)_{\alpha\to 0} &= \frac{1}{2}[g(t_3,t)\delta(t-t_4)\sigma_x\tau_z \\ &\quad - \sigma_x\tau_z\delta(t-t_3)g(t,t_4)]. \end{aligned} \tag{A12}$$

Performing the trace in the Keldysh space we obtain several contributions to the current where, in addition to retarded and advanced GFs, the Keldysh component of the GF is also involved. From Eqs. (4) and (6) we obtain for these GFs,

$$G^K_M = t_R^2G^R_M\hat{V}^\dagger\tau_zG^K_d\tau_z\hat{V}G^A_M, \tag{A13}$$

$$G^K_d = \Gamma_LG^R_d\tau_zg^K\tau_zG^A_d. \tag{A14}$$

We consider the time-averaged transport current. Only the zero multiple of $2eV$ in the Fourier series contributes to the current. In this case we use the Fourier-transform representation of the GFs (A5) and (A6). The current is presented by a trace of proper combinations of these functions in Floquet space. Inserting the expressions Eq. (A11) and (A12) into Eq. (A10), performing the trace in the Keldysh space we arrive at a final form of current in the S-QD-TS (MBS) junction. The total dc current is given by three contributions where for the last two we use Green's functions Eqs. (A13) and (A14),

$$j/j_0 = \frac{t_R^2\Gamma_L}{2\Delta^3}(j_1 + j_2 + j_3), \tag{A15}$$

where $j_0 = e/(2\Delta)$ and j_1, j_2, and j_3 acquire the forms

$$j_1 = \text{tr}\int dE\,\text{Re}\big[G^R_M\bar{V}^+\tilde{G}^R_dg^K\tau_z\tilde{G}^R_d\bar{V}\big], \tag{A16}$$

$$j_2 = \frac{\Gamma_L}{\Delta}\text{tr}\int dE\,\text{Re}\big[G^R_M\bar{V}^+\tilde{G}^R_dg^K\tilde{G}^A_d(g^A\tau_3 - \tau_3g^R)\tilde{G}^R_d\bar{V}\big], \tag{A17}$$

$$j_3 = \frac{\Gamma_L t_R^2}{2\Delta^3}\mathrm{tr}\int dE\,\mathrm{Re}\big[G_M^R\bar{V}^+\tilde{G}_d^R g^K \tilde{G}_d^A\bar{V}G_M^A\bar{V}^+\tilde{G}_d^A \times(g^A\tau_3-\tau_3 g^R)\tilde{G}_d^R\bar{V}\big]. \quad \text{(A18)}$$

Here $\tilde{G}_d^{R,A}=\tau_3 G_d^{R,A}\tau_3$, tr stands for the trace over the Floquet states, and $G_M^{R,A}$ are the matrices in the Floquet basis of dimension $(1+2N)\times(1+2N)$, the same as the blocks $[\bar{V}^+\cdots\bar{V}]$.

This fact is principal: It distinguishes the topological case (with the TS and the MBS) from the trivial normal zero level states inside the gap (here AZBS and Shiba resonance). Indeed the expression for the current in the case of Shiba zero states (i.e., we consider a junction S-QD-S (with the Shiba state) coincides with Eqs. (A17)–(A18) if: (i) We replace Majorana GFs G_M by GFs of Shiba zero states, (ii) drop spinors $\bar{V}^+,\bar{V}$, and (iii) take the trace over the space $4(2N+1)\times 4(2N+1)$.

We also calculate the current in the case of AZBSs. The transport current through the dot in a setup, such as that shown in Fig. 1 of the main text, is described by Eq. (A10) where instead of G_M and Σ we have $G_t=[G_{t0}-\Sigma_g]^{-1}$ and $\Sigma_g=\Gamma_L g_T$ correspondingly, and

$$\frac{\delta\Sigma_g(t_2t_1)}{\delta\alpha(t)}=\Gamma_L\left(\frac{\delta g_T(t_2t_1)}{\delta\alpha(t)}\right)_{\alpha\to 0}. \quad \text{(A19)}$$

With the help of Eqs. (16) and (A19) we obtain

$$j/j_0=\frac{\Gamma_L}{\Delta}\mathrm{tr}\int dE\,\mathrm{Re}\big[G_t^R\tau_z g^K\big(1+\Gamma_L\tilde{G}_t^A g^A\big)\big], \quad \text{(A20)}$$

where $\tilde{G}_t^A=\tau_z G_t^A\tau_z$ and the trace acts in the space $4(2N+1)\times 4(2N+1)$.

[1] A. Y. Kitaev, Phys.-Usp. **44**, 131 (2001).
[2] L. Fu and C. L. Kane, Phys. Rev. Lett. **100**, 096407 (2008).
[3] L. Fu and C. L. Kane, Phys. Rev. B **79**, 161408 (2009).
[4] J. D. Sau, R. M. Lutchyn, S. Tewari, and S. D. Sarma, Phys. Rev. Lett. **104**, 040502 (2010).
[5] R. M. Lutchyn, J. D. Sau, and S. D. Sarma, Phys. Rev. Lett. **105**, 077001 (2010).
[6] Y. Oreg, G. Refael, and F. von Oppen, Phys. Rev. Lett. **105**, 177002 (2010).
[7] J. Alicea, Phys. Rev. B **81**, 125318 (2010).
[8] J. Linder, Y. Tanaka, T. Yokoyama, A. Sudbo, and N. Nagaosa, Phys. Rev. Lett. **104**, 067001 (2010).
[9] J. Alicea, Rep. Prog. Phys. **75**, 076501 (2012).
[10] A. R. Akhmerov, J. Nilsson, and C. W. J. Beenakker, Phys. Rev. Lett. **102**, 216404 (2009).
[11] K. T. Law, P. A. Lee, and T. K. Ng, Phys. Rev. Lett. **103**, 237001 (2009).
[12] Y. Tanaka, T. Yokoyama, and N. Nagaosa, Phys. Rev. Lett. **103**, 107002 (2009).
[13] K. Flensberg, Phys. Rev. B **82**, 180516(R) (2010).
[14] S. Nadj-Perge, I. K. Drozdov, J. Li, H. Chen, S. Jeon, J. Seo, A. H. MacDonald, B. A. Bernevig, and A. Yazdani, Science **346**, 602 (2014).
[15] V. Mourik, K. Zuo, S. M. Frolov, S. R. Plissard, E. P. A. M. Bakkers, and L. P. Kouwenhoven, Science **336**, 1003 (2012).
[16] A. Das, Y. Ronen, Y. Most, Y. Oreg, M. Heiblum, and H. Shtrikman, Nat. Phys. **8**, 887 (2012).
[17] S. Sasaki, M. Kriener, K. Segawa, K. Yada, Y. Tanaka, M. Sato, and Y. Ando, Phys. Rev. Lett. **107**, 217001 (2011).
[18] E. J. Lee, X. Jiang, M. Houzot, R. Aguado, C. M. Lieber, and S. De Franceschi, Nat. Nanotechnol. **9**, 79 (2014).
[19] A. Ueda and T. Yokoyama, Phys. Rev. B **90**, 081405(R) (2014).
[20] C. J. Bolech, and E. Demler, Phys. Rev. Lett. **98**, 237002 (2007).
[21] A. Golub and B. Horovitz, Phys. Rev. B **83**, 153415 (2011); arXiv:1407.5179.
[22] K. Y. M. Blanter and M. Büttiker, Phys. Rep. **336**, 1 (2000).
[23] D. M. Badiane, M. Houzet, and J. S. Meyer, Phys. Rev. Lett. **107**, 177002 (2011).
[24] P. San-Jose, J. Cayao, E. Prada, and R. Aguado, New J. Phys. **15**, 075019 (2013).
[25] G.-Y. Huang, M. Leijnse, K. Flensberg, and H. Q. Xu, Phys. Rev. B **90**, 214507 (2014).
[26] B. Zocher and B. Rosenow, Phys. Rev. Lett **111**, 036802 (2013).
[27] M. Leijnse and K. Flensberg, Phys. Rev. B **84**, 140501(R) (2011).
[28] D. E. Liu and H. U. Baranger, Phys. Rev. B **84**, 201308(R) (2011).
[29] A. Golub, I. Kuzmenko, and Y. Avishai, Phys. Rev. Lett **107**, 176802 (2011).
[30] M. Lee, J. S. Lim, and R. Lopez, Phys. Rev. B **87**, 241402(R) (2013).
[31] M. Cheng, M. Becker, B. Bauer, and R. M. Lutchyn, Phys. Rev. X **4**, 031051 (2014).
[32] R. Chirla, I. V. Dinu, V. Moldoveanu, and C. P. Moca, Phys. Rev. B **90**, 195108 (2014).
[33] D. E. Liu, M. Cheng, and R. M. Lutchyn, Phys. Rev. B **91**, 081405(R) (2015).
[34] J. Nilsson, A. R. Akhmerov, and C. W. J. Beenakker, Phys. Rev. Lett **101**, 120403 (2008).
[35] S. D. Sarma, C. Nayak, and S. Tewari, Phys. Rev. B **73**, 220502(R) (2006).
[36] E. Grosfeld and A. Stern, Proc. Natl. Acad. Sci. U.S.A. **108**, 11810 (2011).
[37] L. Fu and C. L. Kane, Phys. Rev. Lett **102**, 216403 (2009).
[38] T. Hyart, B. van Heck, I. C. Fulga, M. Burrello, A. R. Akhmerov, and C. W. J. Beenakker, Phys. Rev. B **88**, 035121 (2013).
[39] D. E. Liu, Phys. Rev. Lett **111**, 207003 (2013).
[40] S. D. Sarma, J. D. Sau, and T. D. Stanescu, Phys. Rev. B **86**, 220506(R) (2012).
[41] A. Haim, E. Berg, F. von Oppen, and Y. Oreg, Phys. Rev. Lett. **114**, 166406 (2015).
[42] L. P. Kouwenhoven, C. M. Marcus, P. L. McEuen, S. Tarucha, R. M. Westervelt, and N. S. Wingreen, in *Mesoscopic Electron Transport*, edited by L. L. Sohn, L. P. Kouwenhoven, and G. Schön, NATO ASI Series Vol. 345 (Kluwer Academic, Dordrecht, 1997), pp. 105–214.
[43] H. Shiba, Prog. Theor. Phys. **40**, 435 (1968).
[44] A. I. Rusinov, Pi'sma Zh. Eksp. Teor. Fiz. **9**, 146 (1968) [JETP Lett. **9**, 85 (1969)].
[45] L. V. Keldysh, Zh. Eksp. Teor. Fiz. **47**, 1515 (1965).

[46] A. Kamenev and A. Levchenko, Advances in Physics **58**, 197 (2009).
[47] G. B. Arnold, J. Low Temp. Phys. **68**, 1 (1987)
[48] B. Horovitz and A. Golub, Phys. Rev. B **68**, 214503 (2003).
[49] F. Pientka, L. I. Glazman, and F. von Oppen, Phys. Rev.B **88**, 155420 (2013).
[50] P. M. R. Brydon, S. D. Sarma, H.-Y. Hui, and J. D. Sau, Phys. Rev. B **91**, 064505 (2015).
[51] D. Bagrets and A. Altland, Phys. Rev. Lett. **109**, 227005 (2012); A. Altland and M. R. Zirnbauer, Phys. Rev. B **55**, 1142 (1997).
[52] J. Klassen and X.-G. Wen, arXiv:1412.5985.
[53] J. Liu, A. C. Potter, K. T. Law, and P. A. Lee, Phys. Rev. Lett. **109**, 267002 (2012).
[54] S. De Franceschi, L. Kouwenhoven, C. Schönenberger, and W. Wernsdorfer, Nat. Nanotechnol. **5**, 703 (2010).